Numerical modelling of unsteady turbulent flow in smooth-walled pipes

D N Johnston
Department of Mechanical Engineering
University of Bath

Abstract

An efficient numerical model for turbulent friction has been developed for smooth-walled pipe flow. The aim was to develop a new approach to the numerical modelling, eliminating some important approximations and sources of error, such that the method can be applied reliably under a wide range of conditions. A simple two-region model of effective viscosity is used. For short timescales the turbulence level and effective viscosity distribution are 'frozen' in time. The velocity profile is determined numerically for a range of frequencies and viscosity distributions, and this is used to determine the frequency-dependent friction. This is then approximated using simple weighing functions.

This turbulence model can be implemented readily in several types of numerical model for pipe flow, including simple lumped parameter models, finite difference/finite element methods and the Method of Characteristics.

Keywords

Turbulent flow, unsteady flow, weighting functions for unsteady fluid friction, smooth pipes

1. Introduction

Frictional pressure drop characteristics for steady flow in tubes are very well established and reasonably simple both for laminar and turbulent flow. However friction in unsteady flow is rather more complicated [1, 2]. The friction can be considered to be frequency

dependent, and increases with frequency towards an asymptotic gradient of 10 dB/decade and phase of $\pi/4$. That is, it is asymptotically proportional to $\sqrt{j\omega}$ at high frequency. Methods for modelling unsteady laminar friction in the time domain have been developed by Trikha [3], Kagawa et al [4], Vardy and Brown [5] and Johnston [6], amongst others. All of these researchers used a summation of decaying exponential weighting functions to approximate a convolution function which was derived analytically. Because these exponential functions are simply the response of first-order low pass filters, they can be computed very efficiently by recursive means. They are suitable for use with lumped parameter models, the Method of Characteristics (MOC), Transmission Line Method (TLM) and finite element/finite difference methods [6, 7].

However turbulent flow is rather more complicated and not amenable to precise theoretical analysis. Empirical or semi-analytical models need to be used. The intention of this work is not to develop new physical models for turbulence, and the work is based on existing models, using previously justified assumptions. The aim is to develop a new approach to the numerical modelling, eliminating some important approximations and sources of error, such that the method can be applied reliably under a wide range of conditions.

In this paper the focus is on turbulent flow in smooth pipes. The work was done in the context of hydraulic fluid power and aircraft fuel systems, involving small diameter (<5 cm) pipes with low surface roughness, and low to medium Reynolds numbers (up to about 10^5), although the developed model is also applicable in other areas. A companion paper [8] considers turbulent flow in rough pipes.

2. Turbulent friction models

Equations (1) and (2) are the equation of motion and continuity equation [9].

$$\frac{\partial q}{\partial t} + \frac{q}{A}\frac{\partial q}{\partial x} + \frac{A}{\rho}\frac{\partial p}{\partial x} + h(q) = 0 \tag{1}$$

$$\frac{\partial p}{\partial t} + \frac{q}{A}\frac{\partial p}{\partial x} + \frac{\rho c^2}{A}\frac{\partial q}{\partial x} = 0 \tag{2}$$

The second terms may be neglected if $q/A << c$. The last term in equation (1), $h(q)$ represents friction and is dependent on frequency and Reynolds number. For steady flow, the friction term is given by equation (3).

$$h_S(q) = fRe\frac{\nu_F}{2R^2}q \tag{3}$$

The friction factor f can be estimated by Prandtl's universal law of friction for smooth pipes [10], given by equation (4).

$$\frac{1}{\sqrt{4f}} = 2\log_{10}\left(Re\sqrt{4f}\right) - 0.8 \tag{4}$$

Other equations for friction factor could be used, perhaps including roughness effects. Note that, here and throughout this paper, f represents the smaller Fanning friction factor rather than the Darcy friction factor, consistent with the form of Darcy's equation given by equation (5).

$$\Delta P = 4f\frac{L}{2R}\frac{\rho\bar{u}^2}{2} \tag{5}$$

For small variations in q, equations (1) and (2) may be linearised and expressed in the frequency domain by equations (6) and (7).

$$j\omega Q + \frac{A}{\rho}\frac{\partial P}{\partial x} + \frac{\nu_F}{R^2}W(j\omega)Q = 0 \tag{6}$$

$$j\omega P + \frac{\rho c^2}{A}\frac{\partial Q}{\partial x} = 0 \tag{7}$$

$W(j\omega)$ is a frequency-dependent friction function. For laminar flow it can be shown analytically to be given by equations (8) and (9) [1, 2].

$$W(j\omega) = \frac{j\alpha}{\left[\frac{z\,\mathrm{J}_0\left(\sqrt{-j\alpha}\right)}{2\,\mathrm{J}_1\left(\sqrt{-j\alpha}\right)} - 1\right]} \tag{8}$$

where $\alpha = \frac{\omega R^2}{\nu_F}$. (9)

For turbulent flow the friction function also depends on the Reynolds number.

2.1 Instantaneous acceleration based model

A number of researchers have developed an unsteady turbulence model using the so-called 'instantaneous acceleration-based' (IAB) approach. Brunone et al [11] developed an unsteady friction model defined by equations (10) and (11).

$$h(q) = h_S(q) + gAJ_U \tag{10}$$

where $J_U = k\left(\frac{\partial u}{\partial t} - c\frac{\partial u}{\partial x}\right)$. (11)

This was found by Bergant et al [12] to be deficient under certain conditions. They modified it to the form given by equation (12). Pezzinga [13] proposed an alternative given by equation (13).

$$J_U = k\left(\frac{\partial u}{\partial t} - c.\text{sign}(u)\left|\frac{\partial u}{\partial x}\right|\right) \tag{12}$$

$$J_U = k\left(\frac{\partial u}{\partial t} - c.\text{sign}\left(u\frac{\partial u}{\partial x}\right)\frac{\partial u}{\partial x}\right) \tag{13}$$

Various researchers reported excellent results using these models. However Vítkovský et al [14] found that the models performed poorly and under-predicted the friction level for certain transient events, notably valve opening events. These models do not include frequency dependent effects, but results presented by Bergant [12] showed wave attenuation and dispersion (i.e. curvature of the pressure steps) commensurate with frequency-dependent unsteady friction. Vítkovský et al [14] postulated that the apparently good matches obtained by previous researchers might be due to numerical attenuation and dispersion, associated with difficulties in implementing the numerical method. A good match with experimental results does not in itself verify that the model is correct, as modelling and numerical errors can combine to give an apparently good result. The

method has inherent discontinuities which may cause numerical problems. Also, the acceleration component in the friction term results in an effective shift in the speed of sound which causes problems with the MOC grid [15] and necessitates interpolation.

The IAB models are based on empirical considerations [11], whereas the weighting function methods have an analytical basis, albeit with some fairly significant approximations and assumptions. Furthermore the IAB models may not perform well under certain circumstances. The weighting function models can be implemented fairly readily without excessive numerical error. For these reasons, the IAB models are not considered further in this paper, and the focus is exclusively on weighting function models.

2.2 Weighting function models

In a very comprehensive paper, Brown et al [16] developed both a two-layer model and a three-layer model involving laminar, transition and turbulent regions. They showed that the turbulent friction increases with frequency. It tends towards the steady state friction at low frequency, and towards the laminar characteristic at high frequency. Vardy et al [17] developed a similar two-region model, which was developed further as a weighting function model by Taylor et al [18]. Vardy and Brown [19] subsequently improved on their earlier model. In these papers, the frequency-dependent characteristics were calculated using the assumption of invariant or 'frozen' turbulence. That is, the turbulence was represented by an effective viscosity that varied with radius. The viscosity distribution was assumed to remain constant with time. This is probably realistic for high frequencies or very short time scales. However for very low frequencies or long time scales the turbulence or effective viscosity will reach its new equilibrium. Brown et al [16] developed a tentative approximation for the time constant for development of the turbulence level.

Vardy and Brown [19] used a two-region turbulent viscosity profile, with a constant core viscosity and a linearly decreasing viscosity near the wall, using equations (14) and (15).

$$\nu(r) = \nu_C \qquad \text{for } r \le 0.8R \tag{14}$$

$$\nu(r) = \nu_W + 5(\nu_C - \nu_W)\left(1 - \frac{r}{R}\right) \qquad \text{for } r > 0.8R \tag{15}$$

Viscosity ratios are defined by the following equations.

$$\sigma_{CF} = \frac{\nu_C}{\nu_F};\ \sigma_{CW} = \frac{\nu_C}{\nu_W};\ \sigma_{WF} = \frac{\nu_W}{\nu_F} \tag{16}$$

For smooth-walled tubes, the wall viscosity ν_W was assumed to be equal to the fluid viscosity ν_F, so $\sigma_{WF} = 1$ and $\sigma_{CW} = \sigma_{CF}$.

The Laplace transform of the velocity profile in axisymmetric flow is defined by the differential equation

$$sU = -\frac{1}{\rho}\frac{\partial P}{\partial z} + \frac{1}{r}\frac{\partial}{\partial r}\left(r\nu(r)\frac{\partial U}{\partial r}\right) \tag{17}$$

Vardy and Brown [19] developed their model by analytical solution of the flow profile. They solved equation (17) in the constant viscosity core ($r \le 0.8R$). However for the near-wall region ($r > 0.8R$) where the viscosity varies, they assumed planar coordinates (equation (18)) to facilitate the solution.

$$sU = -\frac{1}{\rho}\frac{\partial P}{\partial z} + \frac{\partial}{\partial r}\left(\nu(r)\frac{\partial U}{\partial r}\right) \tag{18}$$

From these solutions the mean velocity, wall shear and friction weighting functions were determined. The weighting functions were then approximated to simpler functions in order to facilitate their inverse Laplace transformation. Vardy and Brown's simplified weighting functions can be expressed in the frequency domain (where $s = j\omega$ and $\alpha = \frac{\omega R^2}{\nu_F}$) by equations (19)-(21).

$$W \approx \frac{fRe}{2} + \frac{2j\alpha}{\sqrt{j\alpha + B^*}} \tag{19}$$

$$B^* = \frac{Re^{\kappa}}{12.86} \tag{20}$$

$$\kappa = \log_{10}\left(\frac{15.29}{Re^{0.0567}}\right) \tag{21}$$

Equations (20) and (21) are more easily represented as a quadratic equation in $\log_{10}(Re)$ as given by equation (22).

$$\log_{10}(B^*) = -0.0567(\log_{10}(Re))^2 + 1.184\log_{10}(Re) - 1.109 \tag{22}$$

Figure 1 shows the weighting functions given by analytical solution of equations (17) and (18) and the approximation given by equations (19) and (22). The functions are plotted against normalised frequency $\alpha_C = \frac{\alpha}{\sigma_{CF}}$, and the magnitude is normalised by dividing by $\sqrt{\sigma_{CF}}$, to compress the range and give the same high frequency asymptotes. The approximation can be seen to introduce some error especially for high σ_{CW}. The maximum magnitude error in the approximation is 1.4:1, and the maximum phase error is 6°.

However if the steady component ($\frac{fRe}{2}$ in equation (19)) is removed, there are large errors in the unsteady component as shown in figure 2. The errors increase with σ_{CW}, with a magnitude error up to 2.4:1, phase error up to 24° and error in the break frequency (assumed to be where the phase = 67.5° or $\frac{3\pi}{8}$ rad) up to 6:1, for σ_{CW} =10^4.

These weighting functions need to be approximated to a series of exponential terms in order to be implemented efficiently in the time domain. Vardy and Brown [5] developed efficient weighting function approximations for laminar and turbulent friction. However this was limited to a single value of Reynolds number for turbulent flow.

Vítkovský et al [20] developed a normalised model for turbulent friction such that the normalised weighting terms were independent of Reynolds number. They did this using Vardy and Brown's approximation in the time-domain, equation (23).

$$w(\tau) = \frac{A^* e^{-B^*\tau}}{\sqrt{\tau}} \approx \sum_{k=1}^{K} m_k e^{-n_k \tau} \tag{23}$$

The weighting function was scaled:

$$w^*(\tau) = \frac{1}{\sqrt{\tau}} \approx \sum_{k=1}^{K} m_k^* e^{-n_k^* \tau} \tag{24}$$

where $m_k^* = {m_k}/{A^*}$, $n_k^* = n_k - B^*$ (25)

In effect they separated the part dependent on Reynolds number (the B^* term) so that the exponential series were independent of Reynolds number. In the frequency domain the weighting function $W^*(j\omega)$ was a straight line with a gradient of -10 dB/decade and a phase of -π/4. In the current paper the weighting function is represented as a function of q whereas Vítkovský et al represented it as a function of $\frac{\partial u}{\partial t}$. Hence there is a factor of $j\omega$ difference between the two representations as well as a scaling factor.

3. Proposed method for modelling unsteady turbulent friction

Vardy and Brown's model [19], and Vítkovský et al's model [20], contained a number of approximations which were necessary due to the difficulty in deriving an analytical expression for the velocity profile and mean velocity, and to facilitate the inverse Laplace transformation of the resultant weighting function. A different approach is used here. The velocity profile and mean velocity are determined numerically in the frequency domain, by numerical integration across the radius. This is done for a range of frequencies, and for a range of ratios of core viscosity to wall viscosity. From this the weighting function is determined as a function of frequency and viscosity ratio. The numerically calculated weighting functions are then approximated by the sum of a series of simpler weighting terms. The inverse Fourier transform of these weighting terms can be calculated easily,

and they can be applied to time domain simulations efficiently. In this way two major approximations are eliminated: firstly the approximation of the near-wall annulus by planar coordinates (equation (18)); and secondly the approximation of the analytically calculated weighting function by the simplified form, equations (19) – (22).

3.1 Calculation of velocity profile

The Fourier transform of the momentum equation for one-dimensional incompressible axisymmetric flow can be expressed by equation (26).

$$j\omega U = S + \frac{1}{r}\left[\frac{\partial}{\partial r}\left(r\nu(r)\right)\frac{\partial U}{\partial r} + r\nu(r)\frac{\partial^2 U}{\partial r^2}\right] \tag{26}$$

S is a forcing term $S = -\frac{1}{\rho}\frac{\partial P}{\partial x}$, and $\nu(r)$ is the effective viscosity which varies with radius. A two-region model similar to that of Vardy and Brown [5, 17] is assumed, with a uniform viscosity ν_C in the core for $0 \le r \le 0.8R$, and with the viscosity decreasing linearly with radius in the outer annulus to the wall viscosity ν_W.

Analytical solution is extremely difficult and probably intractable unless simplifications are made. Instead, in the current work a numerical solution is adopted for $U(r, \omega)$.

The purpose of these calculations was to determine normalised weighting functions as described in section 3.2, and so the dimensions used in the numerical calculations were arbitrary. For simplicity all calculations were done using a radius R = 1m, core viscosity ν_C = 1m^2/s and S = 1m/s^2. Solutions were calculated for a wide range of normalised frequencies α_C and viscosity ratios σ_{CW}. A simple finite difference scheme was adopted to determine U for $0 < r < R$. This results in a tri-diagonal matrix equation which can be solved directly. Details of this are given in Appendix 2.

The flowrate and spatially averaged velocity $\overline{U}$ can be obtained simply by numerical integration of the velocity profile.

Some typical velocity profiles are shown in figure 3(a), for $\sigma_{CW} = 100$ and for different frequencies. The magnitudes are normalised by dividing by the numerically predicted mean velocity, and the phases are relative to *S*. A comparison with analytical results using the solution obtained by Vardy and Brown [19] is shown in figure 3(b). Significant differences between numerical and analytical results are apparent. Only the lower frequency results are shown as the differences become less at high frequency. The differences are due to errors in the analytical model, because of the assumption of planar coordinates for the annular region; numerical errors are negligible and the numerical results can be considered to be practically exact solutions.

For high viscosity ratios σ_{CW} and high frequencies α_C, high shear (i.e. high velocity gradient) occurs in a very narrow annulus near the wall. This can be seen in figure 3(a) for α_C=10^4 and 10^5. To obtain good numerical accuracy it was necessary to use an extremely small grid spacing near to the wall, and to increase the grid spacing smoothly and gradually away from the wall. A model with 2000 grid points and a near-wall spacing of about $10^{-10}R$ was used. This was found to give numerical errors in $\overline{U}$ of less than 0.01%, for normalised frequency α_C up to 10^8 and viscosity ratio σ_{CW} up to 10^5. Fewer grid points could be used; however the numerical calculations are extremely quick and this does not present a problem. Furthermore the efficiency of this numerical integration is unimportant as it is only used to calculate the coefficients for the weighting functions. A user of this model would not have to do this numerical integration as they can use the weighting values presented in table 1.

3.2 Determination of weighting functions

The unsteady friction weighting function can be determined from the numerically calculated mean velocity using equation (27). The steady friction term $(\frac{S}{\overline{u}})$ and the inertance term $(j\alpha_C)$ are subtracted to leave the unsteady friction. Here the weighting function is normalised by $\sqrt{\sigma_{CW}}$ to give the same high frequency asymptote for all σ_{CW}.

$$W_U^*(j\alpha_C) = \left[\frac{S}{\overline{U}(j\alpha_C)} - \frac{S}{\overline{u}} - j\alpha_C \right] \sqrt{\sigma_{CW}} \tag{27}$$

The resulting unsteady weighting functions are shown in figure 4 for a range of α_C and σ_{CW}.

In order to apply this weighting function in time domain numerical simulations, the weighting function may be approximated using a series of weighting terms which are essentially first-order high pass filters. This method is well established for laminar flow [3, 4, 6] and has been extended to turbulent flow [5, 18, 20]. Previous methods have fitted the weighting terms to the simplified approximation, equation (17). However it is proposed here that the weighting terms are fitted directly to the numerically calculated weighting functions, thus eliminating the error inherent in this simplification.

The approximation to the non-dimensionalised weighting function suitable for transformation to the time domain is given by equation (28).

$$W_{UE}^*(j\alpha) = 4 \sum_{k=1}^{K} \frac{m_k^* j\alpha}{n_k^* \sigma_{CF} + j\alpha} \tag{28}$$

The non-dimensional weighting functions W_U^* and W_{UE}^* depend only on non-dimensional frequency α and viscosity ratios σ_{CW} and σ_{CF}. The series of coefficients m_k^* and n_k^* need to be optimised to obtain the best match between the weighting function W_U^* and approximation W_{UE}^*, for a suitable range of frequencies and viscosity ratios σ_{CW}. The approach that was taken was as follows:

1. The n_k^* terms were set to a suitable series of fixed values, to span the required frequency range. Closer spacing would give better accuracy but more terms would be needed for a given bandwidth.

2. For one viscosity ratio, the m_k^* values were optimised by minimising the sum-of-squares relative error over a frequency range $0.01 \le \alpha_C \le 10^8$, with 10 steps per decade of α_C, to obtain the coefficients for that viscosity ratio.
3. Step 2 was repeated for a range of viscosity ratios $1 \le \sigma_{CW} \le 10^5$, with two steps per decade, to obtain a set of coefficients for each viscosity ratio.
4. A quadratic best-fit curve was then fitted to the logarithm of each term, $\log_{10}(m_k^*)$, as a function of $\log_{10}(\sigma_{CW})$.

Optimised coefficients, and quadratic best-fit curves, are shown in figure 5. The quadratic curves fit the optimised coefficient points very closely, within 4%. The coefficients for the quadratic curves are listed in table 1, defined according to equation (29).

$$\log_{10}(m_k^*) = a_2(\log_{10}(\sigma_{CW}))^2 + a_1 \log_{10}(\sigma_{CW}) + a_0 \tag{29}$$

Whilst 12 terms were used in the optimisation, the number of terms needed for a system simulation is generally less than this number. A criterion for selecting the number of terms is described in section 4.

Figure 6 shows the error between the approximated weighting functions W_{UE}^* (obtained from equation (28) using coefficients obtained from the cubic best-fit curves) and the weighting functions W_U^* (obtained by numerical calculation and equation (27)). The errors are small with a maximum amplitude error of 5% and a maximum phase error of 2°. This is likely to be sufficiently accurate. The errors could be reduced further by using a narrower spacing between the n_i^* coefficents and recalculating the weighting coefficients a; however this would require more terms to be used to cover a particular frequency band.

3.3 Determination of core viscosity

In order to use this model it is necessary to estimate the core and wall viscosities. The procedure differs for smooth, transitional and fully rough flow. For smooth flow, the wall

viscosity is equal to the fluid viscosity [19]. Transitional and fully rough flow are dealt with in a companion paper [8].

The core viscosity can be estimated such that the resistance (obtained from numerical solution of equation (26) to estimate the velocity profile for steady state flow) is consistent with Prandtl's universal law of friction, equation (4). Darcy's equation can be rearranged to give equations (30) and (31):

$$S = \frac{4f}{2R}\frac{\overline{u}^2}{2} = \frac{fRe\nu_F\overline{u}}{2R^2} \tag{30}$$

$$\text{or } fRe = \frac{2SR^2}{\overline{u}\nu_F} \tag{31}$$

By numerical solution of equation (26) for $\omega = 0$, arbitrary values of *R,* ν_W and *S,* and a range of values of σ_{CW}, $\overline{u}$ can be determined and fRe can be determined using equation (31). Hence the relationship between fRe and σ_{CW} can be determined. This is shown in figure 7(a) (this graph is to be used to obtain σ_{CW} for a given *fRe*, so fRe is plotted as the abscissa, and σ_{CW} obtained from the ordinate). To reduce the spread of values on the graph σ_{CW} is divided by fRe. The relationship between σ_{CW}/fRe and $\log_{10}(fRe)$ can be approximated to a straight line with a high degree of accuracy (<3% error over the range shown) using equation (32).

$$\frac{\sigma_{CW}}{fRe} \approx 0.1309\log_{10}(fRe) - 0.1119 \tag{32}$$

Results from a number of researchers collected together by Ohmi and Usui [21] showed that the turbulent viscosity in the core lay within the range $0.055 < \frac{\nu_C}{u_* R} < 0.08$ for a range of *Re*, where u_* is the friction velocity, given by $u_* = \sqrt{\frac{\tau_W}{\rho}} = \overline{u}\sqrt{\frac{f}{2}}$. Vardy and

Brown [19] assumed for their two-region model that $N_C = \frac{\nu_C}{u_* R} = 0.065$ for all *Re*. Figure 7(b) shows the variation of N_C calculated using the equation

$$N_C = \frac{\nu_C}{u_* R} = \frac{\sigma_{CW}}{fRe} 2\sqrt{2f} \tag{33}$$

where $\frac{\sigma_{CW}}{fRe}$ is obtained from equation (32) and *f* from Prandtl's universal law of friction for smooth pipes, equation (4).

This gives a value of N_C that tends towards Vardy and Brown's value of 0.065 at high *fRe*, but is significantly lower for low *fRe.* Assumption of a constant value of N_C = 0.065 would give friction factors that are inconsistent with friction factors obtained from Prandtl's universal law of friction.

The discrepancy in N_C may be due to the simple (and probably inaccurate) assumption of a linear variation in turbulent viscosity in the near-wall region. This region has a great influence because the shear rate is very high, but measurements are not available for comparison from this region. To compensate for this, core viscosities lower than those measured by previous researchers [21] need to be used in this model.

The two-region model is a crude approximation and there is insufficient experimental data to verify its accuracy, particularly in the near-wall region. It is possible that future research may result in different distributions of effective viscosity. However the same methods described in this paper could be used. Because the velocity distribution is determined numerically, it would be straightforward to implement for other viscosity distributions. It would then be necessary to perform the optimisation to obtain new coefficients for the weighting functions.

4. Implementation of friction model within an unsteady flow model

The friction can be calculated using the following equation, where y_k are unsteady friction weighting functions.

$$h(t) = fRe' \frac{\nu_F}{2R^2} q(t) + \frac{4\nu_F}{R^2} \sum_{k=1}^{K} y_k(t) \tag{34}$$

The weighting functions y_k can be determined in the time domain by numerical integration. Using the MOC or fixed timestep integration, equation (35) can be used for y [4, 6]

$$y_k(t+\Delta t) = y_k(t) e^{-\left(\frac{n_k \nu_F \Delta t}{R^2}\right)} + m_k \left[q(t+\Delta t) - q(t)\right] e^{-\left(\frac{n_k \nu_F \Delta t}{2R^2}\right)} \tag{35}$$

For variable timestep integration (suitable for lumped parameter models or TLM, FDM and FEM), the weighting functions y_k can be calculated by solution of the differential equation (36).

$$\frac{dy_k}{dt} = m_k \frac{dq}{dt} - \frac{n_k \nu_F}{R^2} y_k \tag{36}$$

The weighting terms m_k and n_k are determined from the normalised values by equations (37) and (38).

$$m_k = m_k^* \sigma_{WF} \sqrt{\sigma_{CW}} \tag{37}$$

$$n_k = n_k^* \sigma_{CF} \tag{38}$$

where for smooth-walled pipe flow, $\nu_W = \nu_F$, so $\sigma_{CF} = \sigma_{CW}$ and $\sigma_{WF} = 1$. All of these values depend on Reynolds number and may need to be constantly updated. This is discussed in the companion paper.

The number of terms K that should be included in the model depends on the bandwidth of the flow and pressure variations. The break frequency for the k_{th} term is given by equation (39).

$$f_k = \frac{n_k^* \nu_F \sigma_{CF}}{2\pi R^2} \tag{39}$$

Generally all terms for which the break frequency is less than the required bandwidth should be included, and in most cases this is unlikely to amount to more than 4-6 terms.

A simple resistance-inertance model can be implemented using equation (40).

$$p_1(t) - p_2(t) = \frac{\rho L}{A}\dot{q}(t) + \frac{\rho L}{A}h(t) \tag{40}$$

Multiple element models can be created readily by chaining this together with compressible volume models. However such models may have poor accuracy and efficiency compared to MOC or TLM models [7]. Implementations in Matlab Simulink of various types of pipeline models incorporating this turbulent friction model are available from Johnston [22].

4.1 Comparison of Models

As an example, the response to a step change in flow was modelled using the Method of Characteristics. The conditions are listed in table 2. A comparison between the proposed model and Vítkovský et al's model [20] is presented in figure 8. The results are of the expected form for a step change. The results for the two models are very similar, with the maximum difference less than 3% and the average difference less than 1% relative to the magnitude of the initial step change. Similar agreement was observed for other conditions. It is reassuring to note that, even though there are significant differences between the models, the results are quite similar. Nonetheless, as a number of sources of error have been eliminated in the proposed model, the user can have more confidence that the results are reliable. Furthermore, whilst eight unsteady friction terms were needed in Vítkovský et al's model to obtain this result, only four terms were needed in the proposed model so the computational demand is lower.

5. Conclusions

An efficient numerical model for turbulent friction in smooth pipes has been developed. The model is based on an effective viscosity profile that was proposed by previous researchers. From this starting point, a different method has been used to develop the numerical approximation. This method eliminates a number of approximations and sources of error in the previous researchers' methods. A simple two-region viscosity model has been used. This is recognised to be simplistic, but the method could readily be applied to different viscosity profiles if required. It would then be necessary to re-evaluate the weighting function coefficients. The model is extended to include the effect of rough walls in the companion paper.

6. References

1 Goodson, R.E., Leonard, R.G., A Survey of Modeling Techniques for Fluid Line Transients, Trans. ASME, J. Basic Eng., June 1972

2 Stecki, J.S. and Davis, D.C., Fluid Transmission Lines - Distributed Parameter models Part 1 - A Review of the State of the Art, Proc. Instn. Mech. Engrs., vol. 200, no. A4, 1986, pp215-228

3 Trikha, A.K., An efficient method for simulating frequency-dependent friction in transient liquid flow. Trans. ASME Journal of Fluids Engineering, Series I, 97, 1975, pp97-105.

4 Kagawa, T., Lee, I., Kitagawa, A. and Takenaka, T., High speed and accurate computing method of frequency-dependent friction in laminar pipe flow for characteristics method, Bull. JSME, Vol. 49, No. 447, 1983, pp2638-2644

5 Vardy, A.E. and Brown, J.M.B., Efficient approximation of unsteady friction weighting functions, Journal of Hydraulic Engineering, v 130, n 11, 2004, pp1097-1107

6 Johnston, D. N., Efficient methods for numerical modeling of laminar friction in fluid lines, Trans. ASME, Journal of Dynamic Systems Measurement and Control, Vol. 128, No. 4, Dec. 2006, pp829-834

7 Soumelidis, M.I., Johnston, D.N., Edge, K.A. and Tilley, D.G., A comparative study of modelling techniques for laminar flow transients in hydraulic pipelines, Sixth JFPS International Symposium on Fluid Power, Tsukuba, 2005.

8 Johnston, D.N., Numerical modelling of unsteady turbulent flow in tubes, including the effects of roughness and large changes in Reynolds number, Submitted to Proc. IMechE, Part C, Journal of Mechanical Engineering Science, 2010

9 Zielke, W., Frequency-Dependent Friction in Transient Pipe Flow, Trans. ASME, J. Basic Eng., 90, 1968, pp. 109–114.

10 Schlichting, H., Boundary Layer Theory, Seventh Edition, McGraw Hill, New York, 1979

11 Brunone, B., Golia, U.M. and Greco, M., Some remarks on the momentum equation for fast transients, Int. Meeting on Hydraulic Transients with Water Column Separation, 9th Round Table of the IAHR Group, Valencia, Spain, 1991, pp201-209

12 Bergant, A., Simpson, A.R. and Vítkovský J., Developments in unsteady pipe flow friction modelling, Journal of Hydraulic Research, Vol. 39, No. 3, 2001, pp249-257

13 Pezzinga, G., Evaluation of unsteady flow resistances by quasi-2D or 1D models, J. Hydraul. Eng., 126(10), 2000, pp778–785.

14 Vítkovský J., Stephens M., Bergant A. and Simpson A., Systematic Evaluation of One-Dimensional Unsteady Friction Models in Simple Pipelines, Journal of Hydraulic Engineering, 2006, pp696-708

15 Brunone, B., Golia, U.M. and Greco, M., Modelling of fast transients by numerical methods, Int. Meeting on Hydraulic Transients with Water Column Separation, 9th Round Table of the IAHR Group, Valencia, Spain, 1991, pp273-280.

16 Brown, F.T., Margolis, D.L. and Shah, R.P., Small Amplitude Frequency Behavior of Fluid Lines with Turbulent Flow, Journal of Basic Eng., Trans. ASME, December, 1969, pp678-692

17 Vardy, A.E., Brown, J.M.B. and Kuo-Lun, H., A weighting function model of transient turbulent friction, Journal of Hydraulic Research, Vol. 31, No. 4, 1993, pp533-548

18 Taylor, S.E.M, Johnston, D.N. and Longmore, D.K., Modelling of transient flows in hydraulic pipelines, Proc IMechE Pt I, vol. 211, no. I6, 1997, 447-456

19 Vardy, A.E. and Brown, J.M.B., Transient turbulent friction in smooth pipe flows, Journal of Sound and Vibration, 259(5), 2003, pp1011-1036

20 Vítkovský J., Stephens M., Bergant A., Lambert M. and Simpson A, Efficient and accurate calculation of Zielke and Vardy-Brown unsteady friction in pipe transients, 9th International Conference on Pressure Surges, Chester, United Kingdom, 24–26 March 2004.

21 Ohmi, M. and Usui, T., Pressure and velocity distributions in pulsating turbulent pipe flow. Part 1, theoretical treatments. Bulletin of JSME, Vol. 19, No. 129, 1976, pp307-313

22 Johnston D. N., Pipeline models in Matlab Simulink, available from http://people.bath.ac.uk/ensdnj/models, accessed Nov 2010

Appendix 1: Notation

$a_0 - a_2$ Coefficients of quadratic function

A Cross-sectional area

A Weighting function term

B Weighting function term

c Speed of sound

f Fanning friction factor

f_k Break frequency of k^{th} weighting term

i Grid point index

k	Weighting function term index
K	Number of weighting function terms
L	Length
m_k	Weighting coefficient
n_k	Weighting coefficient
N	Number of points in numerical model
N_C	Core viscosity coefficient
p	Pressure
P	Laplace or Fourier transform of pressure
q	Flowrate
Q	Fourier transform of flowrate
r	Radial coordinate
R	Bore radius
Re	Reynolds number
s	Laplace operator
S	Forcing term
t	Time
u_*	Friction velocity
U	Laplace or Fourier transform of velocity
$\overline{u}$	Mean flow velocity
$\overline{U}$	Flow velocity (Fourier transform) averaged over the cross-section ($= Q/A$)
w	Friction function
W	Friction function (Fourier transform)
x,y,z	Cartesian coordinates (x = axis of pipe)
α	Non-dimensional frequency ($=\frac{\omega R^2}{\nu_F}$)
α_C	Non-dimensional frequency ($=\frac{\omega R^2}{\nu_C}$)
ν	Kinematic viscosity
ν_C	Effective kinematic viscosity in core

ν_F Kinematic viscosity of fluid

ν_W Effective kinematic viscosity at wall

ρ Density

σ_{CF} Ratio of core to fluid viscosity

σ_{CW} Ratio of core to wall viscosity

σ_{WF} Ratio of wall to fluid viscosity

τ Non-dimensional time ($=\frac{t\nu_F}{R^2}$)

τ_W Wall shear stress

ω Angular frequency

Subscripts

E Approximation

S Steady state

U Unsteady

Superscripts

* Normalised

Appendix 2: Numerical calculation of velocity profile

The velocity profile can be determined by numerical solution of equation (26), reproduced below.

$$j\omega U = S + \frac{1}{r}\left[\frac{\partial}{\partial r}\left(r\nu(r)\right)\frac{\partial U}{\partial r} + r\nu(r)\frac{\partial^2 U}{\partial r^2}\right] \qquad \text{(A1)}$$

As the viscosity distribution is prescribed and is a continuous function, $\frac{\partial}{\partial r}\left(r\nu(r)\right)$ can easily be determined analytically.

At the i_{th} point at radius $r = r_i$, using the notation $U_i = U(r_i)$ for $i = 1$ to N

$$\left.\frac{\partial U}{\partial r}\right|_{r=r_i} \approx \frac{U_{i+1} - U_{i-1}}{r_{i+1} - r_{i-1}} \tag{A2}$$

$$\left.\frac{\partial^2 U}{\partial r^2}\right|_{r=r_i} \approx \frac{\dfrac{U_{i-1}}{r_i - r_{i-1}} - U_i\left(\dfrac{1}{r_i - r_{i-1}} + \dfrac{1}{r_{i+1} - r_i}\right) + \dfrac{U_{i+1}}{r_{i+1} - r_i}}{0.5(r_{i+1} - r_{i-1})} \tag{A3}$$

Equation (A1) can be expressed in finite difference form as

$$aU_{i-1} + bU_i + cU_{i+1} = d \tag{A4}$$

$$a = \frac{\dfrac{\partial}{\partial r}(r\nu(r)) + \dfrac{2r_i\nu(r_i)}{r_i - r_{i-1}}}{r_{i+1} - r_{i-1}} \tag{A5}$$

$$b = -\frac{r_i\nu(r_i)}{r_{i+1} - r_{i-1}}\left(\frac{2}{r_i - r_{i-1}} + \frac{2}{r_{i+1} - r_i}\right) - j\omega r_i \tag{A6}$$

$$c = \frac{-\dfrac{\partial}{\partial r}(r\nu(r)) + \dfrac{2r_i\nu(r_i)}{r_{i+1} - r_i}}{r_{i+1} - r_{i-1}} \tag{A7}$$

$$d = -Sr_i \tag{A8}$$

These apply for $i = 2$ to N-1. At the centre point ($i = 1$, $r_1 = 0$) the boundary condition is $\frac{\partial U}{\partial r} = 0$. However equation (A1) becomes indeterminate at this point. Using Cartesian coordinates (y, z) at this point instead, and since ν is constant in this region,

$$j\omega U = S + \nu\left[\frac{\partial^2 U}{\partial y^2} + \frac{\partial^2 U}{\partial z^2}\right] = S + 2\nu\frac{\partial^2 U}{\partial r^2} \tag{A9}$$

Since $\frac{\partial U}{\partial y} = \frac{\partial U}{\partial z} = \frac{\partial U}{\partial r} = 0$ at (y, z) = (0, 0) or $r = 0$, (A10)

$$\left.\frac{\partial^2 U}{\partial r^2}\right|_{r=0} \approx \frac{2(U_2 - U_1)}{r_2} \tag{A11}$$

so $j\omega U_1 = S + 4\nu_1\left(\frac{U_2 - U_1}{r_2}\right)$ (A12)

At the wall, $U_N = 0$. (A13)

This system of equations can be formed into a tridiagonal matrix equation and solved easily and efficiently.

Captions

Table 1 Quadratic polynomial coefficients and n_k^* values

Table 2 Parameters used in model

Figure 1 Weighting functions including steady component, showing analytical solution of equations (17) and (18), and simplified approximation using equations (19) and (22)

Figure 2 Unsteady weighting functions, showing analytical solution of equations (17) and (18), and simplified approximation using equations (19) and (22)

Figure 3 Predicted velocity profiles for $\sigma_{CW} = 100$, for different frequencies
(a) Numerical approximation
(b) Comparison between numerical model and Vardy and Brown's approximate analytical model

Figure 4 Normalised unsteady weighting functions W_U^* for a range of σ_{CW}

Figure 5 Weighting coefficients (symbols represent optimised value at that value of σ_{CW}; lines represent best-fit quadratic functions)

Figure 6 Error in unsteady weighting function approximations $W_{UE}{}^*$ relative to numerically calculated weighting functions $W_U{}^*$

Figure 7 Variation of σ_{CW} / fRe and N_C with fRe

(a) Variation of viscosity ratio
(b) Variation of N_C

Figure 8 Comparison between proposed model and Vítkovský et al's model for a step change in flowrate

k	a_2	a_1	a_0	n_k^*
1	0.0196466	0.150494	-0.25198	20
2	0.0433595	-0.094614	0.26256	60
3	0.0314749	-0.036212	0.79916	360
4	0.0247278	-0.066953	1.33203	$n_3^* \times 9$
5	0.0126470	-0.037386	1.79049	$n_4^* \times 9$
6	0.0043957	-0.015141	2.25970	$n_5^* \times 9$
7	0.0008864	-0.002871	2.73528	etc
8	0.0001254	-0.000666	3.19317	
9	-0.0000727	0.0010975	3.75574	
10	-0.0001712	-0.0086700	3.98899	
11	0.0007275	0.011337	4.47219	
12	0.0001389	0.0015409	5.39664	

Table 1 Quadratic polynomial coefficients and n_k^* values

Pipe length	20 m
Internal diameter	15 mm
Number of elements	10
Timestep	0.7 ms
Speed of sound	1414 m/s
Density	1000 kg/m^3
Viscosity	3 cSt
Upstream boundary condition	Prescribed pressure: 20 bar
Downstream boundary condition	Prescribed flow step from 1.1 L/s to 1.0 L/s

Table 2 Parameters used in model

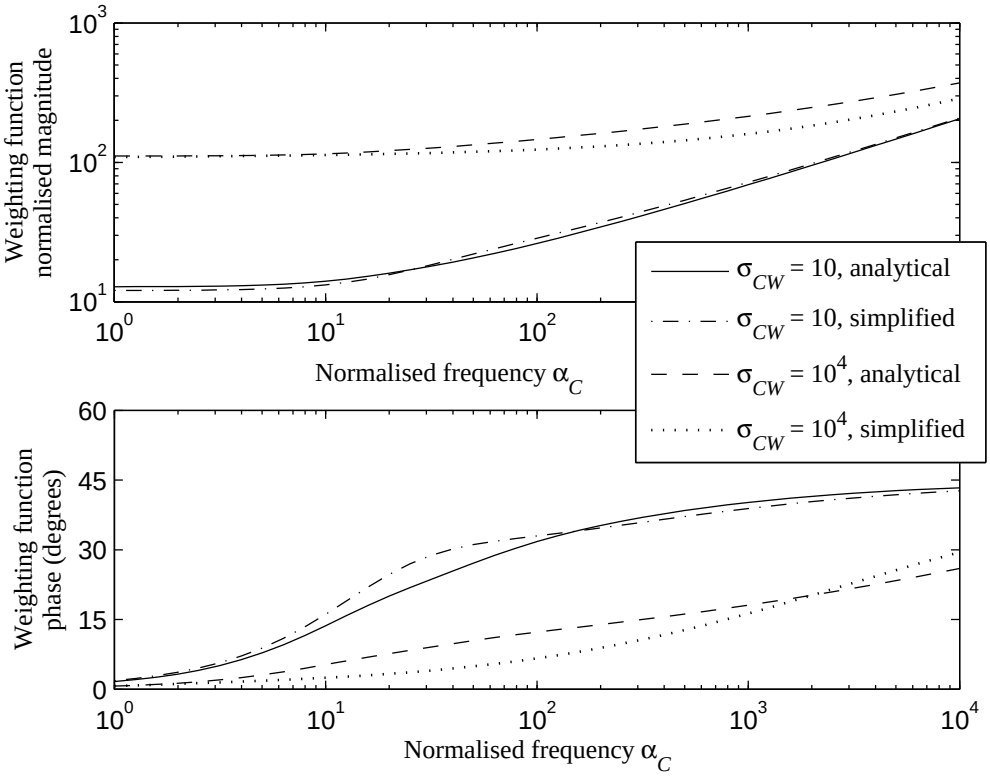

Figure 1 Weighting functions including steady component, showing analytical solution of equations (17) and (18), and simplified approximation using equations (19) and (22)

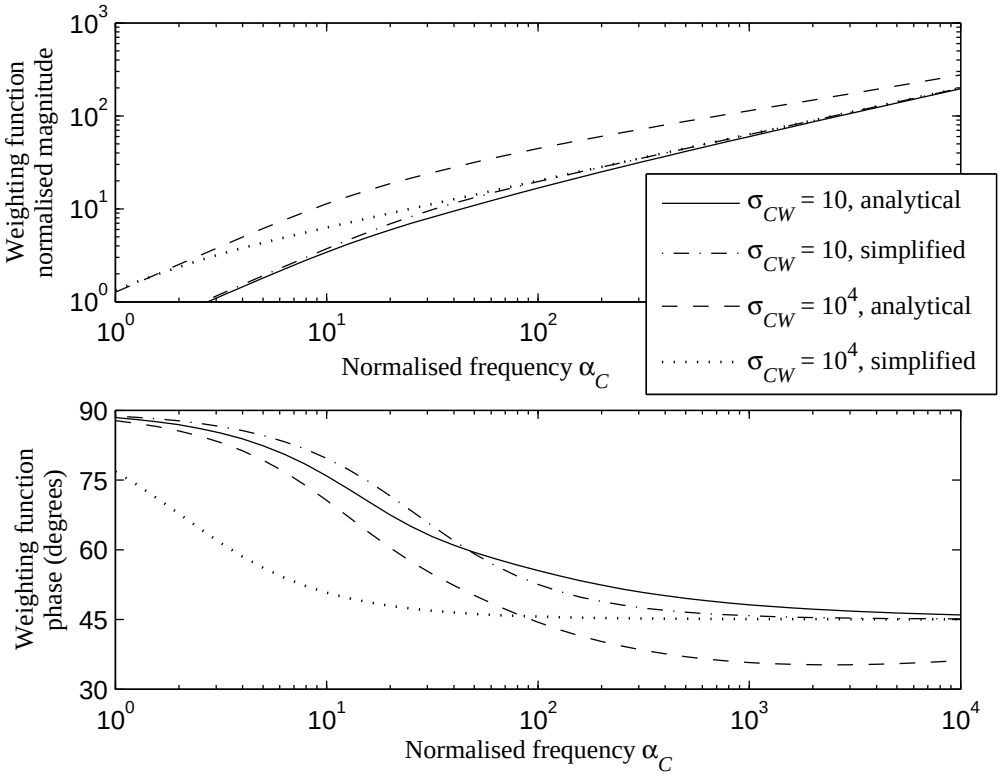

Figure 2 Unsteady weighting functions,
showing analytical solution of equations (17) and (18), and
simplified approximation using equations (19) and (22)

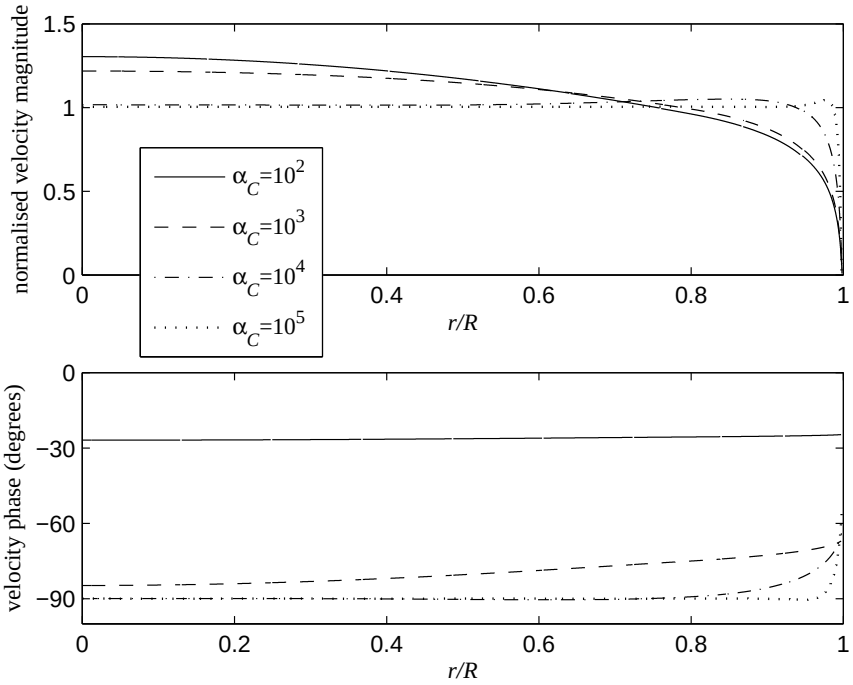

(a) Numerical approximation

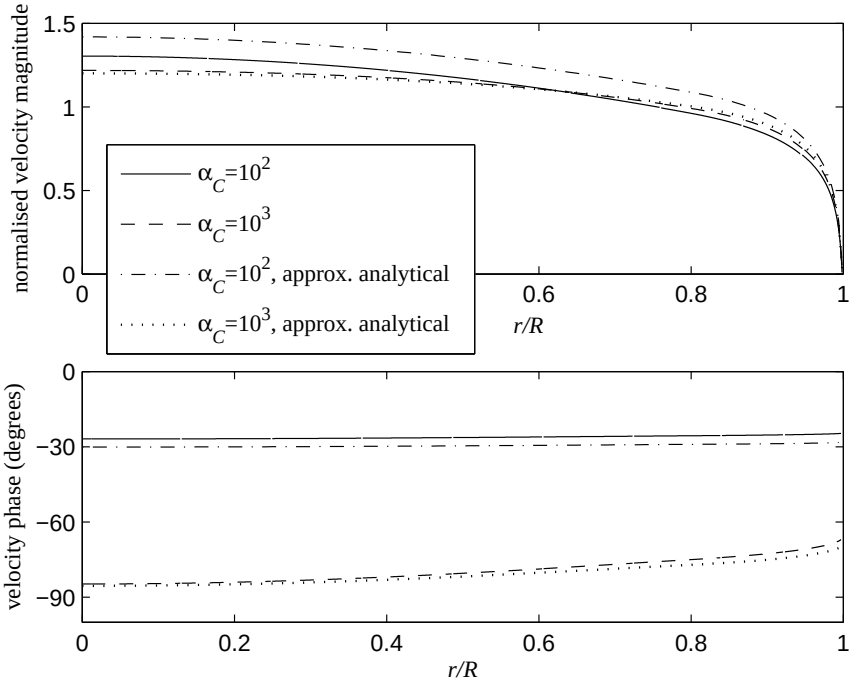

(b) Comparison between numerical model and Vardy and Brown's approximate analytical model

Figure 3 Predicted velocity profiles for $\sigma_{CW} = 100$, for different frequencies

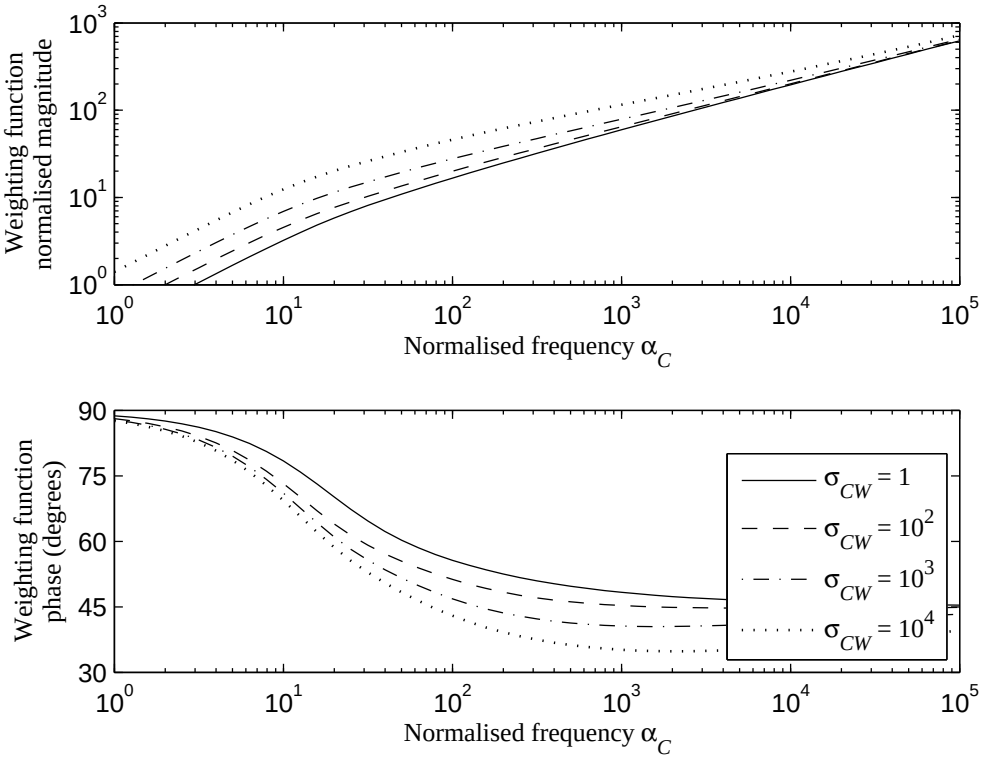

Figure 4 Normalised unsteady weighting functions W_U^* for a range of σ_{CW}

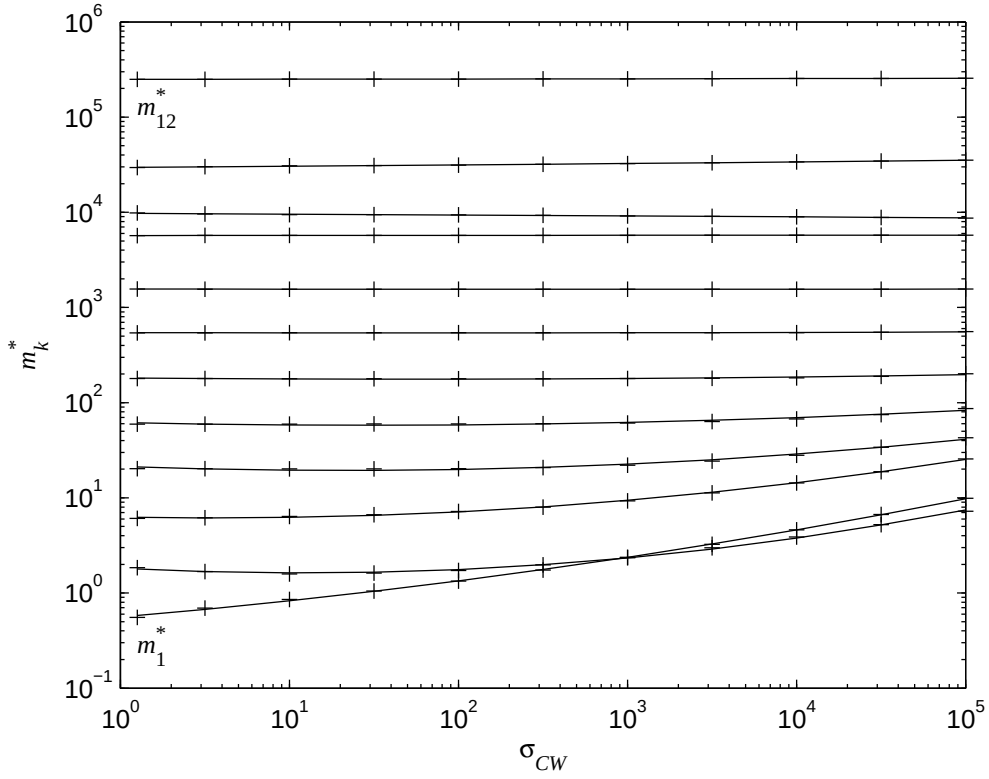

Figure 5 Weighting coefficients (symbols represent optimised value at that value of σ_{CW} ; lines represent best-fit quadratic functions)

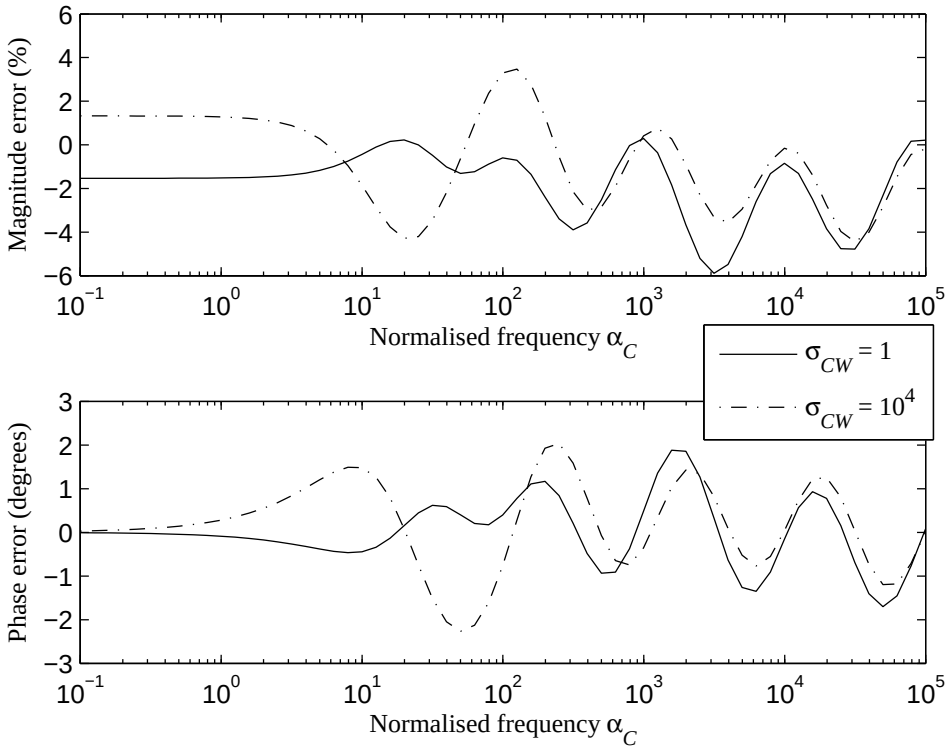

Figure 6 Error in unsteady weighting function approximations W_{UE}^* relative to numerically calculated weighting functions W_U^*

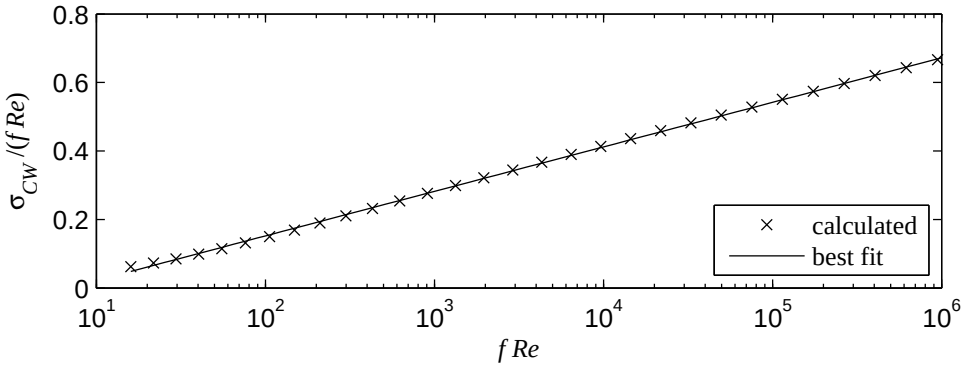

(a) Variation of viscosity ratio

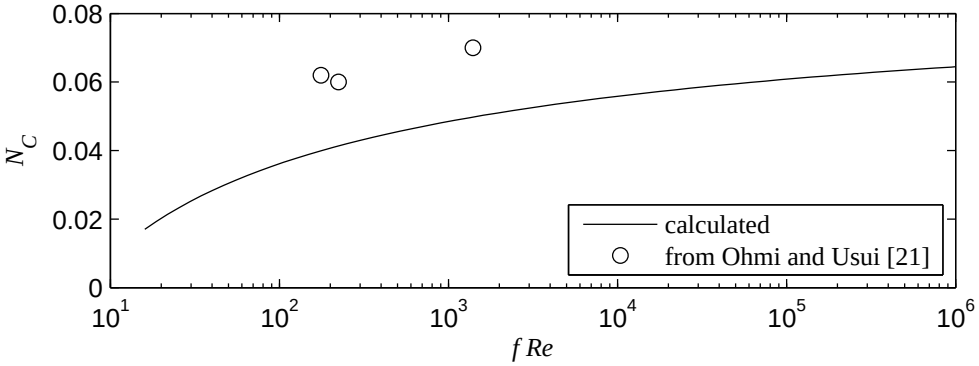

(b) Variation of N_C

Figure 7 Variation of σ_{CW}/fRe and N_C with fRe

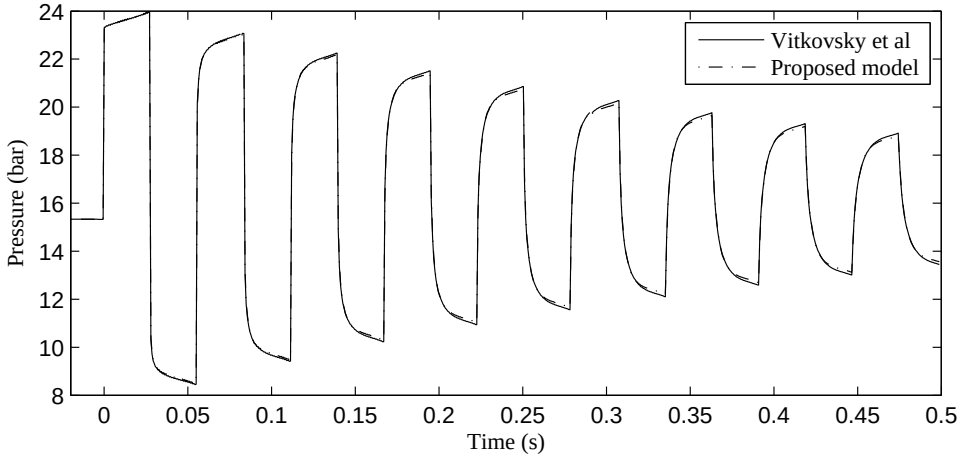

Figure 8 Comparison between proposed model and Vítkovský et al's model for a step change in flowrate